AJNR

The Insula: Anatomic Study and MR Imaging Display at 1.5 T

Thomas P. Naidich, Eugene Kang, Girish M. Fatterpekar, Bradley N. Delman, S. Humayun Gultekin, David Wolfe, Orlando Ortiz, Indra Yousry, Martin Weismann and Tarek A. Yousry

AJNR Am J Neuroradiol 2004, 25 (2) 222-232
http://www.ajnr.org/content/25/2/222

AJNR Am J Neuroradiol 25:222–232, February 2004

The Insula: Anatomic Study and MR Imaging Display at 1.5 T

Thomas P. Naidich, Eugene Kang, Girish M. Fatterpekar, Bradley N. Delman, S. Humayun Gultekin, David Wolfe, Orlando Ortiz, Indra Yousry, Martin Weismann, and Tarek A.Yousry

BACKGROUND AND PURPOSE: **The insula is important for gustatory sensation, motor speech control, vestibular function, and sympathetic control of cardiovascular tone. The purpose of this study was to test two hypotheses: 1) gross anatomic study of the insula will disclose reproducible patterns of insular structure, and 2) analysis of MR appearance will enable physicians to recognize these patterns on imaging studies.**

METHODS: **Gross insular anatomy was determined in 16 normal human cadaveric hemispheres. The 1.5-T MR images of 300 insulae were analyzed to determine the gyral and sulcal patterns displayed; their relationship to the Heschl gyrus, to the overlying opercula, and to the vertical planes perpendicular to the Talairach-Tournoux baseline at the anterior commissure (VAC) and posterior commissure (VPC); their continuity into the orbitofrontal cortex; and appropriate landmarks for the anterior border, apex, and posterior border of the insula.**

RESULTS: **MR images displayed the central sulcus of the insula (97%); the anterior (99%), middle (78%), and posterior (98%) short insular gyri that converge to the apex (100%) anteriorly; and the anterior (99%) and posterior (58%) long insular gyri posteriorly. The middle short gyrus was often hypoplastic (33%). The anterior intersections of the internal and external capsules typically delimit the anterior insular border (87%). VAC intersects the anterior insula (99%), usually at the precentral sulcus. The Heschl gyrus circumscribes the posteroinferior insula (100%). VPC demarcates the posterior insular border (94%).**

CONCLUSION: **The two hypotheses were proved correct. The insula shows reproducible patterns of gross anatomy that are demonstrable on routine clinical MR images obtained at 1.5 T.**

The insula is seen on every MR imaging study of the brain. Familiarity with insular anatomy is important for diagnosis and functional MR imaging, because the insula is the site of the primary gustatory cortex (1), the insular language area (2–4), and significant vestibular integration, including reciprocal visual-vestibular inhibition (5, 6). Infarctions extending to the left insula greatly increase the risk of sudden death from lability of cardiac rhythms and blood pressure because of unbalanced sympathetic tone derived from the right insula (7–10). Detection of insular involvement plays an important role in the diagnosis of diseases such as herpes encephalitis (11, 12), middle cerebral artery infarctions (insular ribbon sign [13], and speech apraxia ([2, 14]). Studies of gross insular anatomy have been reported previously, primarily in the surgical literature (15–24). However, little has been published in the radiologic literature, and little attention has been given to the potential for MR imaging to display the specific gyral and sulcal anatomy of the insula (14).

The purpose of this study was first to analyze the gross anatomy of the insula to identify reproducible patterns and variations of insular anatomy and then to analyze the MR imaging appearance of the insula to determine which anatomic features may be displayed at 1.5 T with clinical MR systems to aid imaging diagnosis.

Methods

This study was conducted after approval by the institution's internal review board. All of the studies were obtained for

Received January 30, 2003; accepted after revision July 7.

From the Departments of Radiology (T.P.N., E.K., G.M.F., B.N.D.) and Pathology, Section of Neuropathology (S.H.G., D.W.), Mount Sinai Medical Center, New York, NY; Department of Radiology, Winthrop University Hospital, Mineola, NY (O.O.); Department of Neuroradiology, Klinikum Grosshadern, Ludwig-Maximilians University of Munich Medical School, Munich, Germany (I.Y., M.W.); Department of Radiology, Medical University, Luebeck, Germany (M.W.); and the Lysholm Radiologic Department, the National Hospital for Nervous Diseases, Queen Square, London, UK (T.A.Y.).

Presented at the 87th annual meeting of the Radiological Society of North America, Chicago, 2001.

Address reprint requests to Thomas P. Naidich, MD, Department of Radiology, Box 1234, Mount Sinai Medical Center, One Gustave Levy Pl, New York, NY 10029.

acceptable clinical purposes. Retrospective image review for determining normal anatomy was judged not to require specific informed consent.

Anatomic Study

Sixteen normal human cerebral hemispheres were obtained at autopsy from patients who had died of unrelated causes. Each specimen was later analyzed pathologically and shown to be normal. The 16 hemispheres were dissected in the sagittal plane by sequential, incremental removal of tissue from the lateral aspect of each hemisphere to expose the insula and to establish the relationship of the insula to the the orbital surface of the frontal lobe and to the overlying opercula. The presence and conspicuity of each gyrus and sulcus of the insula were then determined, as described for the MR imaging study below. The specific anatomic features of each dissection were recorded and documented photographically for later review. The findings in all 16 hemispheres were tabulated to support the subsequent analysis of MR images.

Because variable terminology has been used to describe this anatomy (15–17), herein we specifically adopt the nomenclature of Türe et al (15, 16). The term *central sulcus* (CS) *of the insula* is used to designate the prominent sulcus that angles obliquely across the insula, separating it into anterior and posterior lobules. The term *apex* is used to designate the summit of the pyramid-shaped insula (15). As such, the apex is the point most elevated above the plane of the insula and the point most laterally situated on the insula. The term *pole* is used to identify the most anteroinferior point on the insula. As such, the pole is exclusively a feature of the anterior lobule of the insula and lies anteroinferior to the apex (ie, is subapical) (15–17). The term *sylvian stem* is used to designate the anteriormost portion of the sylvian fissure that originates medially at the anterior perforated substance and then courses laterally, between the orbital surface of the frontal lobe and the temporal pole, to reach the cistern of the insula (15). The term *limen insulae* (threshold to the insula) indicates the band of transitional cortex that extends along the sylvian stem between the anterior perforated substance medially and the gray matter at the pole of the insula laterally. Since this band lies at the inflection point of the sylvian stem, the term limen insulae is also used to indicate the peak of the falciform fold between the frontal lobe superiorly and the insula-temporal lobe posteroinferiorly (15). The new term *pole of the posterior lobule* is introduced to indicate the anteriormost extent of the posterior lobule of the insula where the two long gyri converge to form the posterior wall of the limen insulae.

The anatomy of the opercula is described in accord with standard nomenclature (18, 25–27) (Table 1). Superior to the insula, from anterior to posterior, the portions of the frontoparietal operculum are designated as follows: pars opercularis of the inferior frontal gyrus, inferior end of the precentral gyrus, subcentral gyrus, inferior end of the postcentral gyrus, and supramarginal gyrus. Characteristically, the inferior end of the pars opercularis joins with the inferior end of the precentral gyrus deep to the inferior frontal sulcus, the inferior ends of the precentral and postcentral gyri unite deep to the CS to form the subcentral gyrus, and the supramarginal gyrus of the inferior parietal lobule straddles the posterior ascending ramus of the sylvian fissure to constitute the parietal operculum. Thus, the inferior ends of all these structures join together to form a continuous strip of tissue that abuts onto the insula deep to the surface sulci. Inferior to the insula, the temporal operculum is formed by the superior surface of the temporal lobe (designated the temporal plane), the transverse temporal HG, and the superior temporal gyrus. The HG extends obliquely across the temporal plane from posteromedial to anterolateral, dividing the plane into two parts. The portion of the temporal plane from the temporal pole to the anterior surface of the HG is designated planum polare. The portion of the temporal plane from the posterior surface of the HG to the posterior ascending ramus of the sylvian fissure is designated planum temporale.

TABLE 1: Standard nomenclature and abbreviations

Abbreviation	Structure or Line
PS	Periinsular sulcus
CS	Central sulcus
ASG	Anterior short insular gyrus
MSG	Middle short insular gyrus
PSG	Posterior short insular gyrus
ALG	Anterior long insular gyrus
PLG	Posterior long insular gyrus
HG	Heschl gyrus
MOG	Medial orbital gyrus
POG	Posterior orbital gyrus
PMOL	Posteromedial orbital lobule
AC-PC line	Anterior commissure-posterior commissure baseline (ie, the Talairach-Tournoux baseline)
VAC	Vertical erected perpendicular to the AC-PC baseline at the AC
VPC	Vertical erected perpendicular to the AC-PC baseline at the PC

Also in accord with standard nomenclature (18, 25–27) (Table 1), the portion of the orbital surface of the frontal lobe lateral to the gyrus rectus is said to be formed by four (medial, lateral, anterior, and posterior) orbital gyri arrayed around an H-shaped orbital sulcus. At the posterior medial edge of the orbital surface, the medial and posterior orbital gyri unite to form a prominent posteromedial orbital lobule.

Image Analysis

The institution information system was used to select 200 technically satisfactory, reportedly normal MR imaging studies of the brain obtained with 1.5-T clinical MR systems (Signa; GE Medical Systems, Milwaukee, WI). These studies were restored from the digital archive and reanalyzed on the digital workstation. The first 150 MR images in which no lesions or malformations could be discerned with any of the imaging sequences were accepted as the normal study group. Typical imaging parameters used included sagittal T1-weighted spin-echo sequence: 500/15/1 (TR/TE/excitations), 24-cm field of view (FOV), 4-mm section thickness, 1.5-mm intersection gap, 256 × 192 display matrix; sagittal T2-weighted fast spin-echo sequence: 6000/100/2, echo train length 24, 24-cm FOV, 4-mm section thickness, 1.5-mm intersection gap, 256 × 256 display matrix; axial T2-weighted fast spin-echo sequence: 6000/100/2, echo train length 23, 24 × 18-cm FOV, 5-mm section thickness with 2.5-mm intersection gap, and 256 × 256 display matrix; and axial fluid-attenuated inversion-recovery (FLAIR) sequence: 10,000/160/2200/1 (TR/TE/TI/excitation), 24-cm FOV, 5-mm section thickness with 2.5-mm intersection gap, and 256 × 256 display matrix. These 150 examinations provided 300 hemispheres for imaging analysis, including 146 on sagittal T2-weighted images, four on sagittal T1-weighted images, 147 on axial T2-weighted images, and three on axial FLAIR images.

Each of the 300 MR studies was analyzed for insular topography by two neuroradiologists (T.P.N., E.K.) working cooperatively. In each hemisphere, the CS of the insula was scored as "well seen–complete," "well seen–partial," "poorly seen," or "not seen." The ASG, MSG, and PSG and the ALG and PLG were graded for conspicuity. Easily visualized gyri were scored "well seen." Partially visualized or hypoplastic gyri identifiable in accord with other landmarks were scored "poorly seen." Gyri that could not be visualized were scored "not seen." The PLG was scored "separate" when it was clearly demarcated from the

ALG by a postcentral insular sulcus, even if that sulcus was hypoplastic. The PLG was scored "branched" when it appeared, instead, to represent a short segment arising from the posteroinferior aspect of the ALG. Note was made whether the individual insular gyri were single or bifid, the short gyri converged inferiorly to form the apex, the pole of the insula could be identified in a subapical location, the CS circumscribed the posteroinferior margin of the apex and pole, and the confluence of the ALG and PLG formed the pole of the posterior lobule immediately posterior to the limen insulae. Any hypoplasia of the MSG was specifically recorded. The confluence of the pars opercularis of the inferior frontal gyrus with the inferior precentral gyrus was identified in each case and scored in relation to the adjacent portions of the opercula as "unremarkable," "slightly prominent," or "bulky." The size of this confluence was then analyzed with respect to any hypoplasia of the underlying MSG.

In each subject, the coronal planes perpendicular to the AC-PC line at the AC (VAC) and PC (VPC) (28, 29) were established at the midline and projected onto the insulae laterally. The intersection of the VAC with the insula was scored in relation to the anterior insula as a whole and the specific short gyrus or sulcus at which VAC intersected the superior border of the insula (superior PS). In similar fashion, the projection of the VPC was scored for its relationship to the posterior border of the insula. Specific note was made of the relative positions of the HG (27), of the subcentral gyrus, and of the supramarginal gyrus (26, 30) with respect to the PLG, to each other, and to the posterior border of the insula, by using the VPC as a standard vertical (12–6 o'clock) axis of a clock face.

The axial MR images from the same 300 hemispheres were reviewed to score the conspicuity of the MOG, the POG, the PMOL, and the continuity of the white matter of the PMOL with the extreme capsule (18, 31). The anterolateral aspect of the insula was analyzed in relation to an anterior landmark formed by the junction of the anterior limb of the internal capsule with the external capsule and to a posterior landmark formed by extending the plane of the midline AC to intersect the insulae laterally.

Results

Gross Anatomy

The anatomic group was composed of 10 left and six right hemispheres from eight male and six female cadavers (patients were aged 1 day to 81 years; mean age, 54.7 years). In each case, the base of the insula was delimited by three, well-formed anterior, superior, and inferior PS. The anterior PS measured 20–40 mm (mean, 31.1 mm), the superior PS 25–65 mm (mean, 52.7 mm), and the inferior PS 37–60 mm (mean, 52.1 mm).

In all cases, the junction of the anterior PS with the inferior PS delimited the pole of the insula (Figs 1 and 2); the apex of the insula rose above the surface of the insula, eccentrically close to the pole, to form the point farthest above the plane of the insula (ie, the lateralmost point on the insula); and the pole therefore lay in a subapical position, anteroinferomedial to the apex. The convexity surface of the insula always took the shape of an asymmetric pyramid formed by three faces that met at the apex. From the apex, the anterior face of the pyramid extended down to the anterior PS, the superior face extended down to the superior PS, and the inferior face extended down to the inferior PS. These three faces were covered by the overlying opercula (Fig 3). The anterior face of the insula abutted upon and was covered by the orbitofrontal operculum. The superior face abutted upon and was covered by the frontoparietal operculum, and the inferior face abutted upon and was covered by the temporal operculum (including the transverse temporal HG) (Figs 3 and 4).

In all cases, the CS of the insula crossed the insula obliquely from posterosuperior to anteroinferior and then curved medially to reach the inferior PS and the stem of the sylvian fissure (Fig 1,Table 2). The major segment of the CS divided the insula into a larger anterior lobule and a smaller posterior lobule. The anterior end of the CS passed behind and below the apex of the insula, and then behind and below the pole of the insula, before joining the sylvian stem.

As seen from the front, the anterior face of the insula always displayed two gyri (Figs 1 and 2). The transverse gyrus of the insula extended from the orbital surface of the frontal lobe to the pole of the insula in all cases, and thus lay at the inferiormost aspect of the anterior face. The accessory gyrus of the insula lay superior to the transverse gyrus and formed a "bump" of variable size on the anterior face of the insular pyramid, just superior to the transverse gyrus. In 10 cases, the accessory gyrus was small and remained confined to the anterior face of the insula. In one case, it was prominent but still confined to the anterior face. In five cases, the accessory gyrus was so prominent, it projected laterally to reach the convexity surface of the insula and formed the anteriormost gyrus of the convexity surface.

As seen from the side, the insula was always formed by the convexity surfaces of the anterior and posterior lobules. The ASG, MSG, and PSG typically formed the larger anterior lobule, whereas the ALG and PLG formed the smaller posterior lobule (Fig 1). The number of gyri presenting at the convexity surface of the insula varied substantially, however, because of the variable prominence of the accessory gyrus and variable hypoplasia of each short and long insular gyrus. In these 16 specimens, the convexity surface displayed four gyri (two anterior, two posterior) in one case, five gyri (three anterior, two posterior) in 10 cases, and six gyri (four anterior, two posterior) in five cases.

Anterior Lobule.—The ASG usually formed the first (anteriormost) gyrus on the convexity surface of the anterior lobule. When the acessory gyrus was small (62.5%), the ASG formed, as well, the portion of the anterior face of the insula above the accessory gyrus. When the accessory gyrus was large (31%), the accessory gyrus formed nearly all the anterior surface of the pyramid and bulged laterally to form the first gyrus on the convexity surface of the anterior lobule. In these cases, the ASG was displaced posteriorly.

The MSG was the most variable gyrus of the anterior lobule. The MSG was approximately coequal in size with the ASG in nine cases, but hypoplastic in five cases, and not identifiable in two cases. The MSG was often depressed below the convexity surface of the insula when the overhanging frontoparietal operculum was formed by especially prominent gyri (nine

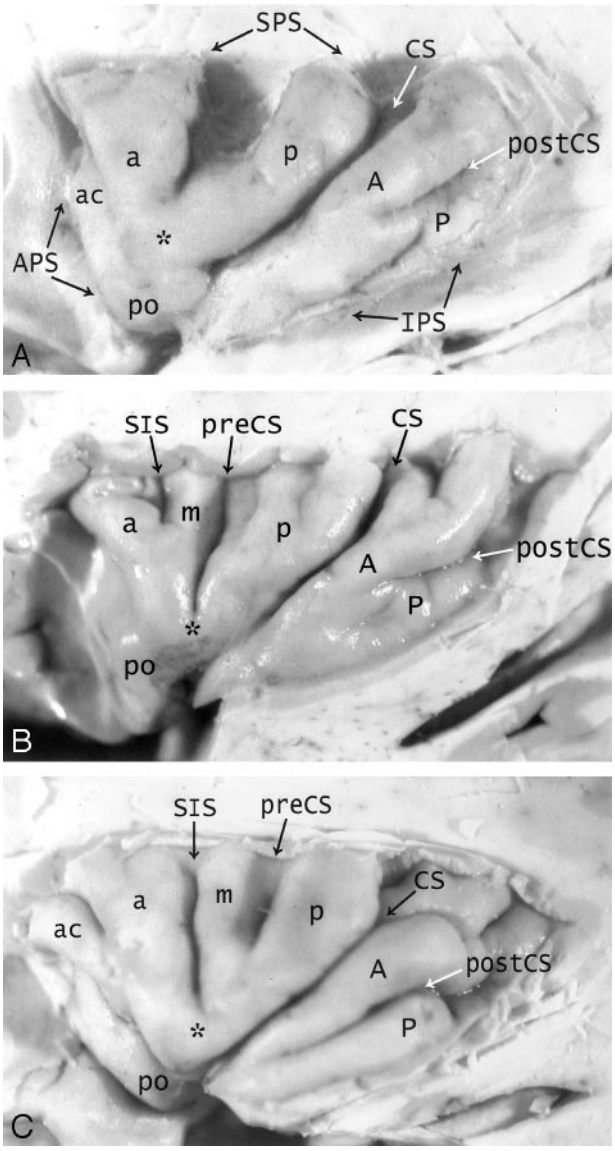

FIG 1. *A–C*, Anatomy of the convexity surface of the left insular lobe after resection of the overlying opercula, vessels, and pia-arachnoid. Gross anatomic specimens from a 50-year-old woman (*A*), a 63-year-old man (*B*), and a 71-year-old man (*C*). The anterior PS (*APS*), superior PS (*SPS*), and inferior PS (IPS) define the base of the insular lobe. The oblique CS of the insula subdivides the insula into larger anterior and smaller posterior lobules.

Anterior lobule: The ASG (*a*), MSG (*m*), and PSG (*p*) form most of the convexity surface of the anterior lobule. The short insular sulcus (*SIS*) separates ASG from MSG. The precentral sulcus (*preCS*) separates MSG from PSG. MSG shows variable size and depression below the surface of the insula. The number of gyri on the convexity surface of the anterior lobule varies substantially: two in *A*, three in *B*, and four in *C*. The apex (asterisk) of the insula forms by the convergence of the inferior ends of some or all of the short gyri. In *A*, the apex is formed only by the ASG and PSG, with no contribution from the hypoplastic MSG (most frequent type). In *B* and *C*, all three short gyri contribute to the apex. The pole (*po*) of the insula lies at the most anteroinferior point on the insula, near to but separate from the apex. The accessory gyrus (*ac*) forms a variable portion of the upper anterior face of the anterior lobule and, when large, may contribute to the convexity surface as well. In *A*, a prominent accessory gyrus (*ac*) projects anterior to the ASG, but does not reach to the convexity surface of the insula. In *C*, a very large accessory gyrus (*ac*) projects laterally to form the anteriormost gyrus on the convexity surface of the anterior lobule. The transverse gyrus forms the lower portion of the anterior face of the insula (see Fig 2).

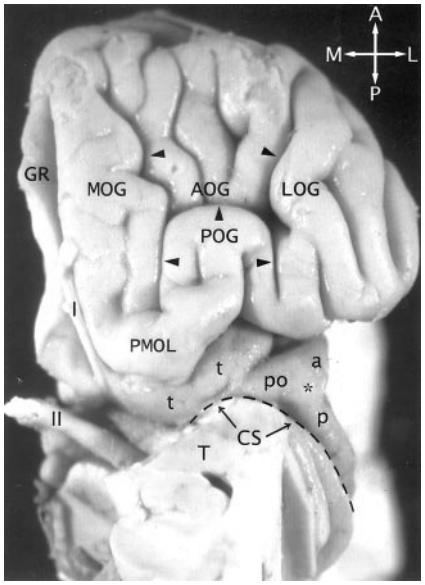

FIG 2. The transverse gyrus and the orbitofrontal insula relationship. Base view of the orbital surface of the left frontal lobe after resection of part of the gyrus rectus (*GR*) and the anterior portion of the temporal lobe (*T*). Medial is to the reader's left. *I* indicates olfactory bulb; *II*, optic chiasm and tract. The H-shaped orbital sulcus (arrowheads) defines the MOG, POG, anterior orbital gyrus (*AOG*), and lateral orbital gyrus (*LOG*). At the posteromedial aspect of the orbitofrontal surface, the posterior portion of the MOG merges with the medial portion of the POG to form the prominent PMOL. PMOL gives rise to the transverse insular gyrus (*t*) that extends laterally to form the pole (*po*) of the insula just anteroinferomedial to the apex (asterisk) of the insula. The CS (dashed line) curves inferiorly immediately behind and below the apex and the pole en route to join the stem of the sylvian fissure. The ASG (*a*) and the PSG (*p*) converge to form the apex of the insula anterior to the CS. In this image, the deliberate slight rotation used to illustrate the course of the transverse gyrus from the PMOL to the pole also rotates the apex medially, so the apex does not appear to lie as far lateral in position as it would in a true base view.

cases, including two in which the MSG was equal to the ASG in size).

The PSG formed the precentral gyrus of the insula immediately anterior to the CS in all cases. Typically, the short insular sulcus separated the ASG from the MSG, whereas the precentral sulcus of the insula separated the MSG from the PSG (Table 2). In one case with absent MSG, the short insular sulcus and the precentral sulcus merged completely, so they could not be identified as separate structures.

The apex of the insula was formed by the short gyri in all cases, but the specific pattern of the short gyri and the contribution of each short gyrus to the apex were variable (Fig 1). The ASG contributed to the apex in 13 cases, the MSG in seven cases, the PSG in

Posterior lobule: The ALG (*A*) and the PLG (*P*) form the posterior lobule. In *C*, the ALG and PLG are well defined and completely separated by a complete postcentral sulcus (*postCS*). In *A* and *B*, the ALG and PLG are incompletely separated by shallow or incomplete postcentral sulci (*postCS*). In *B*, the dominant ALG forms the pole of the posterior lobule at the limen, while the PLG appears to branch off the posterior inferior aspect of the ALG. The superior ends of many of the insular gyri are bifid.

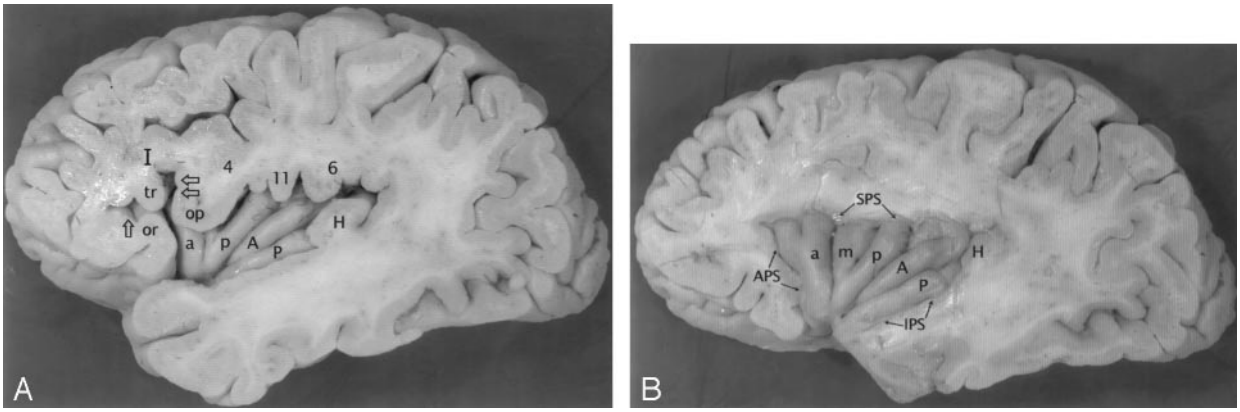

FIG 3. *A* and *B*, Anatomic relationship of the opercula to the insula at earlier (*A*) and later (*B*) stages of dissection of the left cerebral hemisphere of a gross anatomic specimen from a 71-year-old man. The partes orbitalis (*or*), triangularis (*tr*), and opercularis (*op*) of the inferior frontal gyrus (*I*) overlie the anterior lobule of the insula. The anterior horizontal ramus (single open arrow) of the sylvian fissure leads to the anterior PS (*APS*). The anterior ascending ramus (dual open arrows) of the sylvian fissure leads to the superior PS (*SPS*) (*8*). The pars opercularis (*op*) joins with the inferior end of the precentral gyrus (*4*) to form most of the frontal operculum. In this specimen, they form a "bulky" union that invaginates into the convexity surface of the anterior lobule and depresses the MSG (*m*) slightly below the surface of the insula. Further posteriorly, the subcentral gyrus (*11*) and the anterior limb of the supramarginal gyrus (*6*) form the rest of the frontoparietal operculum that overlies the posterior lobule. The HG (*H*) overlies the PLG (*P*), so the anteromedial surface of HG abuts onto the lateral surface of the PLG. Deeper dissection (in *B*) shows the origin of the HG immediately posterior to the insula, posterosuperolateral to the PLG. In this specimen, the postcentral sulcus defines separate ALG (*A*) and PLG (*P*). PLG is dominant and forms the pole of the posterior lobule at the limen.

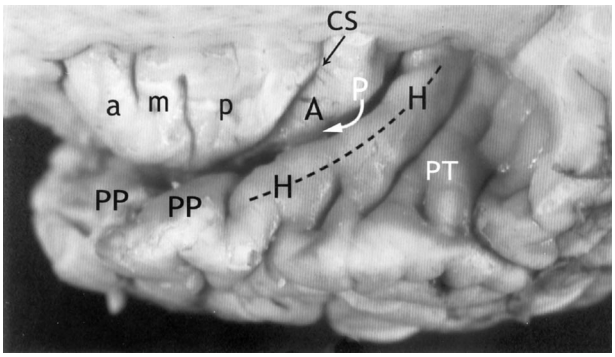

FIG 4. Relationship of the insula to the temporal operculum. Gross anatomic specimen from a 44-year-old woman, viewed from above and lateral after removal of the frontal and parietal opercula to expose the superior surfaces of the ASG (*a*), MSG (*m*), PSG (*p*), the CS, and the ALG (*A*). The HG (*H*) arises immediately posterior to the insula and curves anterolaterally around the lateral surface of the PLG (*arrow*), largely obscuring it in this view. The anteromedial surface of the HG abuts upon and conforms to the surface of the PLG as it crosses the superior surface of the temporal lobe. *PP* indicates planum polare; *PT*, planum temporale.

11 cases, and the accessory gyrus in one case. Most frequently, the apex was formed by the ASG + PSG, with no contribution from a hypoplastic MSG (seven cases, 44%). Other patterns seen at the apex were ASG + MSG + PSG (two cases), ASG + MSG (two cases), MSG + PSG (two cases), ASG alone (one case), MSG alone (one case), and ASG + accessory gyrus (one case). The apex was grooved by inferior extension of the short sulcus in six cases, by inferior extension of the precentral sulcus in six cases, and by the accessory sulcus in one case. The pole of the insula was grooved by the short sulcus in one case and by the accessory sulcus in one case.

Posterior Lobule.—The ALG was complete in 13 cases (Figs 1 and 3). In the other three cases, a variant course of the postcentral sulcus truncated the ALG, leaving only a short posterior segment designated partial ALG. The PLG was complete in nine cases (Fig 1C), incomplete in six cases, and barely present in one case. The incomplete forms of the PLG resembled a posteriorly directed "outgrowth" from the back of the ALG, so the combined ALG + PLG took a "branched" configuration in each of these six cases (Fig 1A and B). The postcentral sulcus of the insula was well seen and complete in all nine cases where the PLG was well defined and complete, variably complete in the six cases with partial PLG, and almost indetectable in the single case of nearly absent PLG.

The gyri of the posterior lobule of the insula converged to form the pole of the posterior lobule behind the limen insulae in all cases. In five cases, the ALG was dominant and isolated the PLG away from the limen. In two cases, the PLG was dominant and isolated the ALG apart from the limen (Fig 3B). In nine cases, the ALG and PLG were nearly equal in their contribution (with ALG extending anterior to PLG in three of the nine cases, and the PLG extending anterior to the ALG in six of the nine cases).

Operculum.—The HG arose immediately posterior to the PLG in all cases. The proximal posterior portion of HG always curved around and "hugged" the inferior aspect of the PLG, until HG extended too far laterally to lie against the insula (Fig 4). The subcentral and supramarginal gyri formed the frontoparietal operculum overhanging the posterior lobule in all cases.

Imaging Series

The MR imaging study group included 100 female and 50 male subjects ranging in age from 2 months to 96 years (mean age, 39.3 years.) By decade (D), the subjects were distributed as follows: D1, 6%; D2,

TABLE 2: Gross anatomic features of 16 formalin-fixed normal human insulae

Insular Gyri and Sulci	Well Seen–Complete	Well Seen–Incomplete/Partial/Hypoplastic	Poorly Seen	Not Seen
CS	94 (15)	6 (1)	-	-
Anterior surface of insula				
Transverse gyrus	100 (16)	-	-	-
Accessory gyrus	100 (16)	-	-	-
Convexity surface; anterior lobule of insula				
ASG	94 (15)	6 (1)	-	-
MSG	56 (9)	31 (5)	-	12 (2)
PSG	94 (15)	6 (1)	-	-
SIS	75 (12)	12 (2)	6 (1)	6 (1)
PIS	75 (12)	19 (3)	-	6 (1)
Convexity Surface: posterior lobule of insula				
ALG	81 (13)	19 (3)	-	-
PLG	56 (9)	38 (6)	6 (1)	-
PostCS	56 (9)	38 (6)	6 (1)	-
Overhanging opercula				
HG	100 (16)	-	-	-
Subcentral gyrus	100 (16)	-	-	-
Supramarginal gyrus	100 (16)	-	-	-

Note.—Data are percentages (number of specimen). SIS indicates short insular sulcus; PIS, precentral insular sulcus.

TABLE 3: Display of insular anatomy on sagittal MR images

	Left Hemisphere (n = 150)				Right Hemisphere (n = 150)			
Insular Gyri and Sulci	Well Seen	Poorly Seen	Not Seen	Bifid	Well Seen	Poorly Seen	Not Seen	Bifid
ASG	99.3 (149)	0.7 (1)	0 (0)	7.3 (11)	100 (150)	0 (0)	0 (0)	13.3 (20)
MSG	82 (123)	11.3 (17)	6.7 (10)	0 (0)	74 (111)	13.3 (20)	12.7 (19)	1.3 (2)
PSG	97.3 (146)	2 (3)	0.7 (1)	2 (3)	99.3 (149)	0.7 (1)	0 (0)	8 (12)
ALG	98.7 (148)	1.3 (2)	0 (0)	10 (15)	99.3 (149)	0.7 (1)	0 (0)	21.3 (32)
PLG	59.3 (89)	20.7 (31)	20 (30)	0 (0)	57.3 (86)	18.7 (28)	24 (36)	0 (0)
CS	78.7 (118)*	18 (27)	3.3 (5)	NA	86.7 (130)*	10 (15)	3.3 (5)	NA
HG	100 (150)	0 (0)	0 (0)	NA	100 (150)	0 (0)	0 (0)	NA

Note.—Data are percentages (number of hemispheres). NA indicates not applicable.

* Data presented are the sum of well seen–complete and well seen–partial.

10%; D3, 18.7%; D4, 18%; D5, 15.3%; D6, 13.3%; D7, 10%; D8, 8%; D9, 0%; and D10, 0.7%.

Sagittal MR Images

The conspicuities of the individual gyri and sulci are detailed in Table 3. The CS provided a prominent landmark on conventional sagittal T1- and T2-weighted MR images in 96.7% of patients (Figs 5 and 6). The ASG and PSG were nearly always well seen, but the MSG was demonstrated less often and less well. The inferior portions of these short gyri could be seen to converge toward the apex of the insula in each case. The ALG was well displayed far more often than was the PLG. In most cases, the two long gyri exhibited the "branched" configuration (64% of left hemispheres, 60.7% of right hemispheres) (Fig 1B and 6B). In each case with a branched configuration, the PLG appeared shorter than the ALG, leaving a posterior "gap" that was filled in by the HG. The two long gyri were distinguished as wholly separate gyri in only 16 left hemispheres (10.7%) and 17 right hemispheres (11.3%) (Figs 1C and 6A). The specific gyral configuration of the PLG could not be clearly characterized in 38 left hemispheres (25.3%) and 42 right hemispheres (28%).

Overlying Opercula.—The frontal operculum overlay the anterior lobule of the insula in all cases (Figs 5 and 6). The junction of the pars opercularis of the inferior frontal gyrus with the inferior precentral gyrus was classified as bulky in 120 (40%) of 300 hemispheres. This "bulky configuration" showed a partial correlation with hypoplasia of the MSG and depression of the MSG beneath the surface of the insula. In those hemispheres with hypoplastic MSG, the junction was bulky in 34 (64%) of 53 left and 34 (72%) of 47 right hemispheres (Fig 7).

The subcentral and supramarginal gyri formed the parietal operculum overlying the posterior lobule (Figs 5 and 6). These gyri demonstrated variable position relative to the HG. Viewing all sagittal images with anterior oriented toward the analyst's left, and using the VPC as the vertical 12–6 o'clock axis of a clock face, the supramarginal gyrus usually lay posterosuperior to the HG at 1–2 o'clock (left 87.7%,

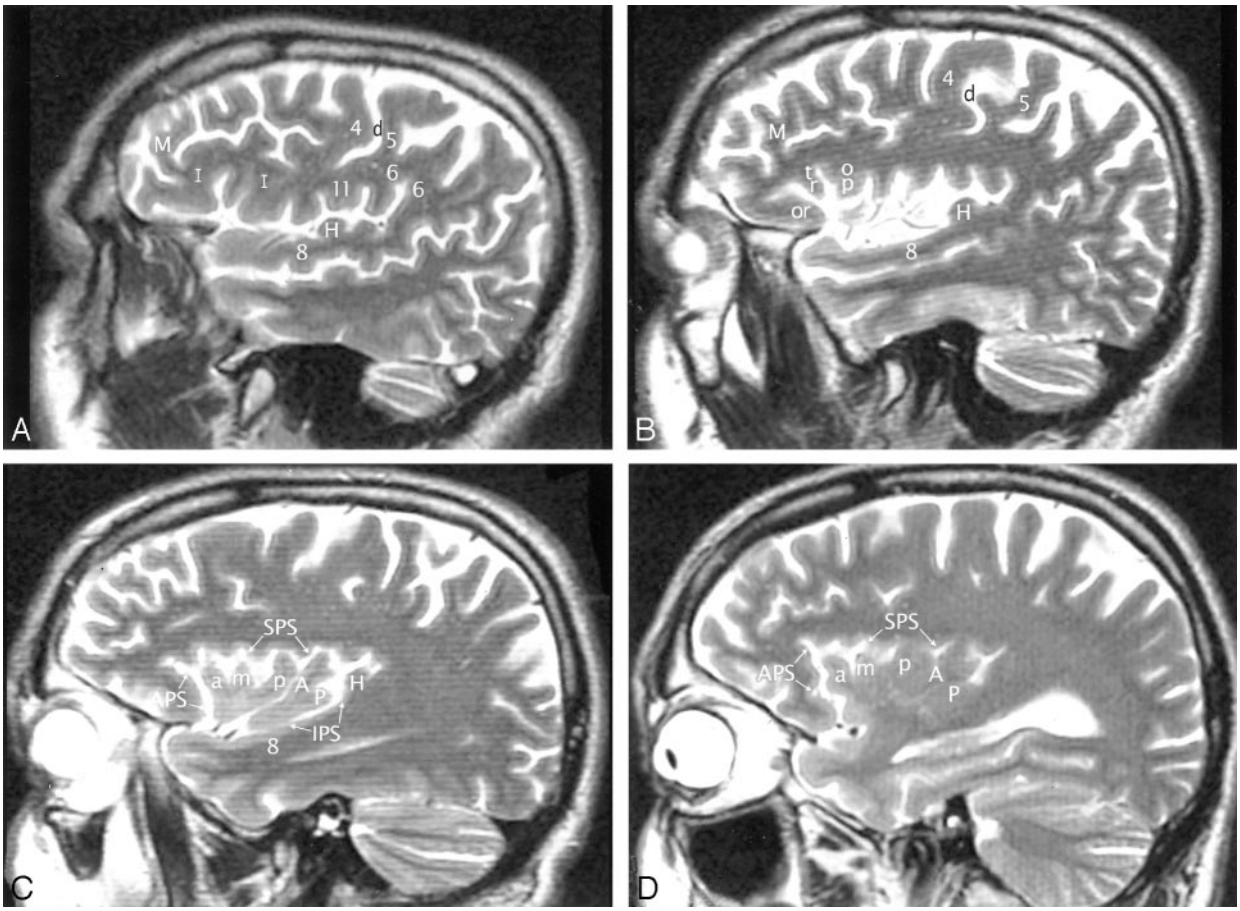

FIG 5. *A–D*, Imaging anatomy of the normal insula in a 51-year-old man. Sequential sagittal T2-weighted MR imaging sections from lateral (*A*) to medial (*D*) demonstrate the anterior (*APS*), superior (*SPS*), and inferior (*IPS*) PS, the ASG (*a*), MSG (*m*), and PSG (*p*) of the larger anterior lobule, and the ALG (*A*) and the branched configuration of the PLG (*P*) of the smaller posterior lobule. The CS (*d*) courses across the convexity between the precentral gyrus (*4*) and the postcentral gyrus (*5*) and then curves across the insula between the corresonding gyri of the insula (ie, between *p* and *A*). The overlying opercula interdigitate with the insular gyri with no significant distortion of insular anatomy. The HG (*H*) lies immediately behind the PLG and marks the posteroinferior border of the insula. *M* indicates middle frontal gyrus; *I*, inferior frontal gyrus; *6*, supramarginal gyrus; *8*, superior temporal gyrus; and *11*, subcentral gyrus. Other abbreviations as in Figs 1–4.

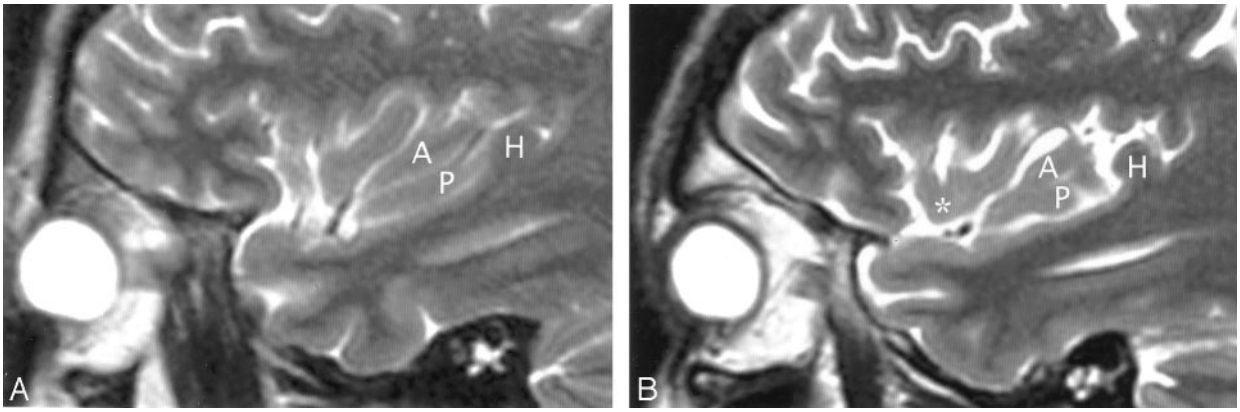

FIG 6. *A* and *B*, Imaging anatomy of the posterior lobule on sagittal T2-weighted MR images in a 13-year-old girl (*A*) and a 26-year-old man (*B*). In *A*, the ALG (*A*) and PLG (*P*) are well formed and distinct, correlating with Fig 1C. In B, ALG (*A*) and PLG (*P*) are poorly separated. PLG appears to bud off the posterior aspect of the ALG, giving the posterior lobule a branched configuration, such as seen in Fig 1B. Note the convergence of the short insular gyri to form the apex (asterisk in *B*) as seen in Fig 1B, the course of the CS posteroinferior to the apex en route to the stem of the sylvian fissure, the relationship of the pole of the posterior lobule to the limen, and the relationship of the HG (*H*) to both the PLG and the entire posterior lobule.

right 78.3%). The subcentral gyrus lay anterosuperior to the HG, anywhere along an arc extending from 10 o'clock (left 45.5%, right 48.1%) through 11 o'clock (left 29.9%, right 30.2%) to 12 o'clock (left 16.8%, right 12.3%) with respect to HG.

The temporal operculum immediately posterior

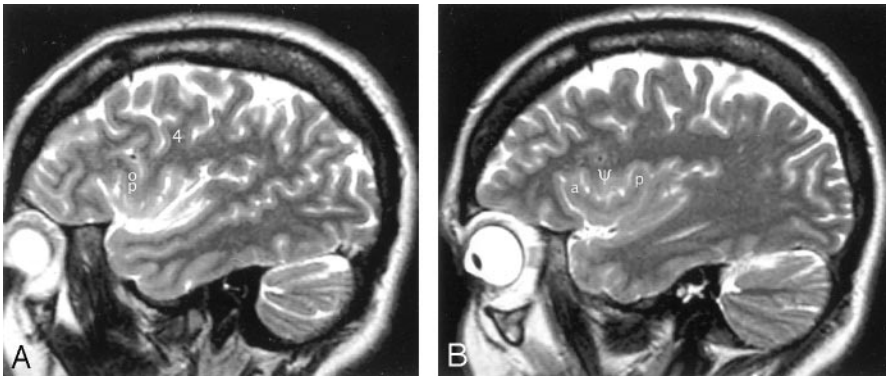

FIG 7. *A* and *B,* Sagittal T2-weighted MR images of the left hemisphere in a 34-year-old woman show the opercular-insular relationship. The union of the pars opercularis (*op*) of the inferior frontal gyrus with the inferior end of the precentral gyrus (*4*) forms a very bulky "pseudomass" (Ø) that invaginates into the convexity surface of the anterior lobule, depresses the insular surface at the MSG, and splays the ASG (*a*) apart from the PSG (*p*). (See also Figs 1 and 3.)

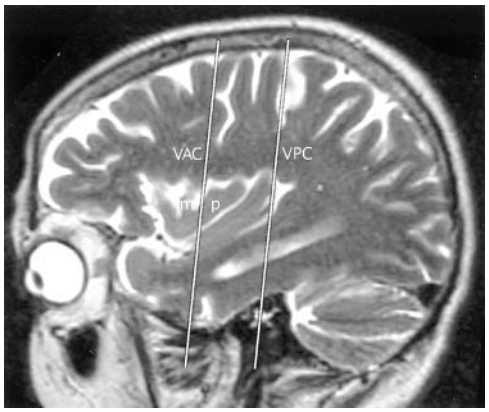

FIG 8. Talairach-Tournoux relationship of the insula. Sagittal T2-weighted MR image in a 26-year-old woman. The two vertical white lines indicate the insular intersections of the coronal planes erected perpendicular to the AC-PC baseline at AC (*VAC*) and at PC (*VPC*). VAC nearly always intersects the anterior lobule, most frequently in relation to the upper portion of the precentral sulcus between the MSG (*m*) and the PSG (*p*). VPC typically defines the posterior margin of the insula.

TABLE 4: Intersection of the coronal plane VAC and VPC with the insula on sagittal MR images

Line and Intersection	Left Hemisphere (n = 150)	Right Hemisphere (n = 150)
VAC line		
Anterior lobule	99.3 (149)	99.3 (149)
Anterior to ASG	0 (0)	0 (0)
ASG	0 (0)	0 (0)
ASG/MSG	1.3 (2)	0.7 (1)
MSG	23.3 (35)	24 (36)
MSG/PSG	58 (87)	50.7 (76)
PSG	16.7 (25)	24 (36)
CS	0.7 (1)	0.7 (1)
VPC line		
Defines posterior insula	93.3 (140)	95.3 (143)
Anterior to posterior insula	5.3 (8)	4 (6)
Posterior to posterior insula	1.3 (2)	0.7 (1)

Note.—Data are percentages (number of hemispheres). ASG/MSG indicates short insular sulcus; MSG/PSG, precentral insular sulcus.

and lateral to the PLG was formed by the HG in all cases (Figs 5 and 6). Therefore, the anterior surface of the most medial portion of HG marked the posterior border of the insula.

Relationship of VAC and VPC to the Insula

The VAC.—The lateral extension of the coronal plane at VAC intersected the upper border of the anterior insula in all but one hemisphere on each side (due to patient rotation) (Fig 8, Table 4). Most frequently, VAC intersected the insula over the precentral sulcus between the MSG and PSG, next most commonly over the MSG itself, and less commonly over the PSG.

The VPC.—The coronal plane at VPC defined the posterior limit of the insula in 94% of all hemispheres (Table 4). When the VPC lay in a different position, the difference could be attributed to patient rotation in seven of 10 left hemispheres and four of seven right hemispheres. In these cases, the direction of patient rotation could readily be predicted simply from the position of the VPC with respect to the posterior border of the insula.

Axial MR Images

In nearly all cases (99%), the MOG and the POG were seen to form the PMOL, and the white matter of the PMOL was shown to be directly continuous with the extreme capsule deep to the insula (Figs 2 and 9). The apex of the insula was seen as a laterally directed prominence at the anterolateral insular cortex in more than 90% of hemispheres. In nearly all of these, the apex was bracketed, anteriorly and posteriorly, between the coronal "planes" through the intersections of the anterior limbs of the internal capsules with the anteriormost external capsules, and the midline portion of the AC (Fig 9). The plane through the junctions of the internal and external capsules also defined the anterior border of the insula in 87% of cases (Table 5). In the other cases, the cistern of the insula appeared to extend far anterior to this line, deep to the inferior frontal gyrus, along the anterior horizontal or anterior ascending rami of the sylvian fissure.

Discussion

The insula was first described by Reil (1809) (15, 19). Since then, detailed descriptions of gross insular

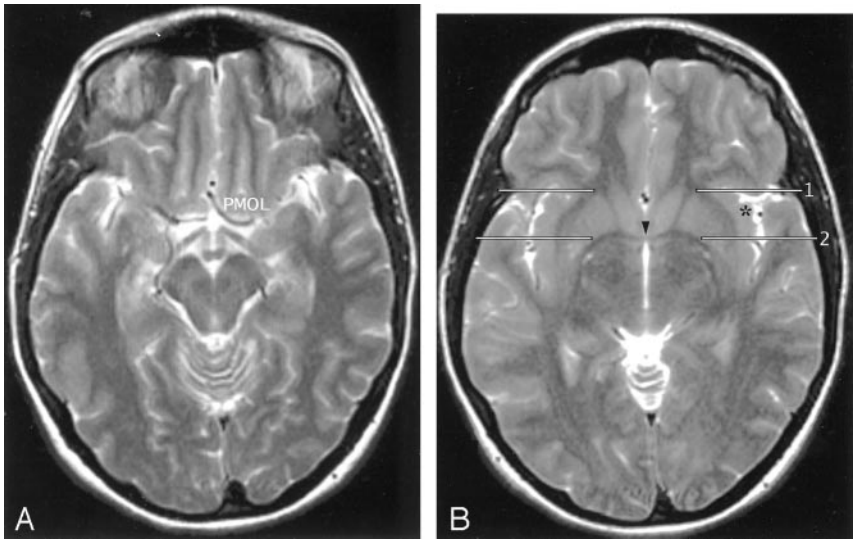

FIG 9. *A* and *B*, Axial T2-weighted MR images in the AC-PC plane. The MOG and POG converge to form the PMOL at the anterolateral aspect of the suprasellar cistern. The white matter of the orbitofrontal lobe continues directly around the sylvian fissure into the extreme capsule deep to the insular cortex. In axial sections obtained along the AC-PC plane, the coronal plane (*1*) through the junction of the anterior limb of the internal capsule with the external capsule on each side provides one landmark for the anterior border of the insula on each side. The coronal plane (*2*) through the midline portion (arrowhead) of the AC (VAC) intersects the anterior insula. The apex (asterisk) of the insula lies between these two planes. The coronal plane through the PC (not shown) defines the posterior margin of the insula.

TABLE 5: Display of orbitofrontal and insular anatomy on axial MR images

Feature	Left Hemisphere (n = 150)		Right Hemisphere (n = 150)	
	Yes	No	Yes	No
MOG	100 (150)	0 (0)	100 (150)	0 (0)
POG	100 (150)	0 (0)	100 (150)	0 (0)
Posteromedial orbital lobule	98.7 (148)	1.3 (2)	99.3 (149)	0.7 (1)
Continuity of white matter from the orbitofrontal to the insular lobes	98.7 (148)	1.3 (2)	98.7 (148)	1.3 (2)
Apex shown as a laterally directed prominence	92 (138)	8 (12)	90.7 (136)	9.3 (14)
Apex bracketed between the anterior plane through the junctions of the anterior limbs of the internal capsules with the anteriormost external capsules and the posterior plane at VAC	95.7 (132/138)	4.3 (6/138)	98.5 (134/136)	1.5 (2/136)
Anterior plane defines the anterior border of the insula	86 (129)	14 (21)	88.7 (133)	11.3 (17)

Note.—Data are percentages (number of hemispheres).

anatomy, of insular vasculature, and of surgical approaches to the insula have been published, most recently by Türe et al (15, 16), Varnavas and Grand (17), Zentner et al (20), and Duffau et al (21). These publications provided the impetus to learn the gross anatomy of the insula and then analyze its MR imaging appearance. Increasing utilization of the Talairach-Tournoux (AC-PC) baseline and the coronal planes VAC and VPC (28) to correlate anatomy with the functional data from positron emission tomography and functional MR imaging (31–37) prompted use of the AC-PC baseline for the axial MR images and analysis of the insular intersections of VAC and VPC in the imaging portion of the study.

This study documents that many substantial insular features may be displayed and identified reproducibly with clinical MR imaging at 1.5 T. Variations in the gyri and sulci are numerous, but follow familiar patterns that permit their identification on MR images. Significant insular features may be delimited by use of landmarks such as the CS, HG, VAC, VPC, and the junction of the internal and external capsules anteriorly. The understanding gained through this study enhances interpretation of MR images.

The confluence of the pars opercularis with the inferior precentral gyrus has been shown to be very prominent in 40% of insulae. Approximately two-thirds of insulae with hypoplasia of the MSG show such "bulky" opercular confluence (Fig 7). This interrelationship could explain the lower position of the second loop of the sylvian triangle commonly observed at angiography (38). To our knowledge, this is the first potential explanation to be offered for this well-known angiographic curiosity.

Literature review supports the anatomic observations made in this study. As in this study, the total number of insular gyri observed in other series has varied from four to seven (average, five) and has often differed from side to side in the same patient (15, 17, 22). Reviewing 53 hemispheres, Varnavas and Grand (17) found five insular gyri in 90.5%, six in 3.8%, and seven in 1.9%. In all of these cases, the additional gyri were limited to the anterior lobule. Two hemispheres (3.8%) showed only four insular gyri (one hemisphere with two anterior and two posterior gyri, and one hemisphere with three anterior gyri and one PLG). No study has shown more than two gyri in the posterior lobule of the insula.

The relationships between the insula and the coronal planes used as landmarks in this study could contribute to our understanding of the folding of the brain surface during development. Embryologically, the cerebral hemispheres represent diverticular outpouchings of the alar plate of the prosencephalon that overlap and then adhere to the lateral surfaces of the diencephalon (39). The opercula represent further expansions of the pallium to overlap the insula. In this context, it is intriguing that the coronal plane through the anterior junctions of the internal and external capsules so often defines the anterior extent of the insula, that the coronal plane through the PC (VPC) defines the posterior edge of the insula, and that the apex of the insula falls between the VAC and the anterior junctions of the internal and external capsules. These coronal planes could reflect structural lines or lines of tension that influence the pattern of folding, and provide baselines for studying that folding during development.

Insular Function

Important insular functions include gustatory sensation, motor planning of speech, vestibular function, and sympathetic/parasympathetic balance of cardiovascular function.

Primary Gustatory Cortex.—The primary gustatory area lies in the anterior insula or at the base of the CS (1). Naming olfactory stimuli activates the left insula (although simple olfactory stimulation does not) (40). Damage to the right insula produces deficits in recognizing taste stimuli presented on the ipsilateral side of the tongue (41). Damage to the left insula causes deficits in recognizing taste stimuli presented on either the ipsilateral or the contralateral side of the tongue (41). This effect could be the result of injury to the gustatory cortex itself or to cortex needed to name the gustatory sensations.

Insular Language Area.—The left anterior insula is necessary for formulating an articulatory plan (3). Lesions of the precentral gyrus of the left insula disrupt planning and initiation of articulation, causing speech apraxia (2, 14). The true Broca area may lie within the left anterior insula, not the inferior frontal gyrus (3, 4). Conversely, the right anterior insula becomes activated during vocal repetition of nonlyrical tunes, suggesting that different, complementary networks subserve nonlyrical singing (right) and speaking (left) (42).

Cardiopulmonary Regulation.—In humans, stimulation of the left insula increases parasympathetic tone, whereas stimulation of the right insula predominantly increases sympathetic tone (7). Amytal inactivation of the left hemisphere increases heart rate, but amytal inactivation of the right hemisphere does not (8). Damage to the left insula may shift cardiovascular balance toward increased basal sympathetic tone (favoring arrythmias) and thereby contribute to the increased cardiac mortality known to accompany acute left insular stroke (30). Increasing evidence indicates that the insula plays a crucial role in cerebrogenic cardiovascular and autonomic disturbances, including disturbances in the electrocardiogram, elevation of cardiac enzymes, cardiac arrythmias, disturbed blood pressures, cerebrogenic pulmonary edema, and sudden death in patients with subarachnoid hemorrhage, intracerebral hemorrhage, and ischemic stroke (7–10).

Vestibular Function.—Stimulation of the vestibular system by caloric irrigation with ice water or by galvanic stimulation of the mastoid activates the contralateral posterior insula and deactivates the visual association cortices (BA 18 and 19) (5, 6). Stimulation of the vestibular system visually (optokinetic stimulation) activates the same areas of the posterior insula. If, however, the subject fixes on the scene visually, the optokinetic response is suppressed and does not activate the insulae (5). That is, the brain appears to receive sensory input from both the vestibular and the visual systems, and routinely uses reciprocal inhibitory visual-vestibular interactions to suppress discordant data from whichever system is not in current use (6). Since the insulae also serve as sensory areas for esophageal stimulation and motor areas for vomiting, using visual fixation to suppress vestibular function may explain how staring at the horizon successfully suppresses motion sickness.

The anatomic relationships demonstrated by MR imaging may be used to localize the sites of insular abnormality. It is hoped that, in the future, improved interpretation of clinical MR images of insular abnormality will permit precise correlation of anatomy with clinical abnormality in individual patients and thereby extend our understanding of insular function.

Conclusion

The two hypotheses were proved correct. Dissection of human hemispheres disclosed reproducible anatomic features of the insula that were well displayed and easily appreciable on clinical MR images obtained at 1.5 T. More precise characterization of insular anatomy may potentially lead to improved interpretation of functional MR imaging studies that activate the insula, and thus of insular function.

References

1. Ogawa H **Gustatory cortex of primates: anatomy and physiology.** *Neurosci Res* 1994;20:1–13
2. Dronkers NF. **A new brain region for coordinating speech articulation.** *Nature* 1996;384:159–161
3. Wise RJ, Greene J, Buchel C, Scott SK. **Brain regions involved in articulation.** *Lancet* 1999;353:1057–1061
4. Price CJ. **The anatomy of language: contributions from functional neuroimaging.** *J Anat* 2000;197:335–359
5. Dieterich M, Brandt T. **Vestibular system: anatomy and functional magnetic resonance imaging.** *Neuroimaging Clin N Am* 2001;11: 263–273
6. Brandt T, Bartenstein P, Janek A, Dieterich M. **Reciprocal inhibitory visual-vestibular interaction: visual motion stimulation deactivates the parieto-insular vestibular cortex.** *Brain* 1998;121:1749–1758
7. Oppenheimer S. **The anatomy and physiology of cortical mechanisms of cardiac control.** *Stroke* 1993;24(suppl I): I-3–I-5
8. Zamrini EY, Meador KJ, Loring DW, et al. **Unilateral cerebral inactivation produces differential left/right heart rate responses.** *Neurology* 1990;40:1408–1411

9. Oppenheimer SM, Kedem G, Martin WM. **Left-insular cortex lesions perturb cardiac autonomic tone in humans.** *Clin Auton Res* 1996;6:131–140
10. Cheung RTF, Hachinski V. **The insula and cerebrogenic sudden death.** *Arch Neurol* 2000;57:1685–1688
11. Kissane JM. **Anderson's pathology.** Vol 2, 9th ed. St Louis: CV Mosby, 1990:2160–2161
12. Jordan J, Enzmann DR. **Encephalitis.** *Neuroimaging Clin N Am* 1991;1:17–38
13. Truwit CL, Barkovich AJ, Gean-Marton A, Hibri N, Norman D. **Loss of the insular ribbon: another early CT sign of acute middle cerebral artery infarction.** *Radiology* 1990;176:801–806
14. Nagao M, Takeda K, Komori T, Isozaki E, Hirai S. **Apraxia of speech associated with an infarct in the precentral gyrus of the insula.** *Neuroradiology* 1999;41:356–357
15. Türe U, Yaşargil DCH, Al-Mefty O, Yaşargil MG. **Topographic anatomy of the insular region.** *J Neurosurg* 1999;90:720–733
16. Türe U, Yaşargil MG, Al-Mefty O, Yaşargil DCH. **Arteries of the insula.** *J Neurosurg* 2000;92:676–687
17. Varnavas GG, Grand W. **The insular cortex: morphological and vascular anatomic characteristics.** *Neurosurgery* 1999;44:127–138
18. Ono M, Kubick S, Abernathy CD. *Atlas of the Cerebral Sulci.* New York: Thieme Medical Publishers, Inc. 1990
19. Reil 1809. Cited by: Türe U, Yaşargil DCH, Al-Mefty O, Yaşargil MG. **Topographic anatomy of the insular region.** *J Neurosurg* 1999; 90:720–733
20. Zentner J, Meyer B, Stangl A, Schramm J. **Intrinsic tumors of the insula: a prospective surgical study of 30 patients.** J Neurosurg 1996;85:263–271
21. Duffau H, Capelle L, Lopes M, Faillot T, Sichez J-P, Fohanno D. **The insular lobe: physiological and surgical considerations.** *Neurosurgery* 2000;47:801–811
22. Augustine JR. **The insular lobe in primates including humans.** *Neurol Res* 1985;7:2–19
23. Augustine JR. **Circuitry and functional aspects of the insular lobe in primates including humans** *Brain Res Brain Res Rev* 1996;22: 229–244
24. Watkins KE, Paus T, Lerch JP, et al. **Structural asymmetries in the human brain: a voxel-based statistical analysis of 142 MRI Scans.** *Cereb Cortex* 2001;11:868–877
25. Duvernoy H. *The Human Brain. Surface, Three Dimensional Sectional Anatomy and MRI.* New York: Springer-Verlag, 1991
26. Naidich TP, Valavanis AG, Kubik S. **Anatomic relationships along the low-middle convexity, I: normal specimens and magnetic resonance imaging.** *Neurosurgery* 1995;36:517–532
27. Yousry TA, Fesl G, Büttner A, Noachtar S, Schmid UD. **Heschl's gyrus: anatomic description and methods of identification on magnetic resonance imaging.** *Intl J Neuroradiol* 1997;3:2–12
28. Talairach J, Tournoux P. *Co-Planar Stereotaxic Atlas of the Human Brain. 3-Dimensional Proportional System. An Approach to Cerebral Imaging.* Rayport M, trans. New York, Thieme, 1988
29. Zilles K, Schlaug G, Geyer S, et al. **Anatomy and transmitter receptors of the supplementary motor areas in the human and nonhuman primate brain.** Adv Neurol 1996;70:29–43
30. Naidich TP, Brightbill TC. **Systems for localizing fronto-parietal gyri and sulci on axial CT and MRI.** *Int J Neuroradiol* 1996;2:313–338
31. Naidich TP, Grant JL, Altman N, et al. **The developing cerebral surface: preliminary report on the patterns of sulcal and gyral maturation–anatomy, ultrasound, and magnetic resonance imaging.** *Neuroimaging Clin N Am* 1994;4:201–240
32. Steinmetz H, Seitz RJ. **Functional anatomy of language processing: neuroimaging and the problem of individual variability.** *Neuropsychologia* 1991;29:1149–1161
33. Freund HJ. **Functional organization of the human supplementary motor area and dorsolateral premotor cortex.** *Adv Neurol* 1996;70: 263–269
34. Burton DB, Chelune GJ, Naugle RI, et al. **Neurocognitive studies in patients with supplementary sensorimotor area lesions.** *Adv Neurol* 1996;70:249–261
35. Amunts K, Zilles K. **Advances in cytoarchitectonic mapping of the human cerebral cortex.** *Neuroimaging Clin N Am* 2001;11:151–169
36. Weismann M, Yousry I, Heuberger E, et al. **Functional magnetic resonance imaging of human olfaction.** *Neuroimaging Clin N Am* 2001;11:237–250
37. Alkadhi H, Crelier GR, Boendermaker SH, et al. **Reproducibility of primary motor cortex somatotopy under controlled conditions.** *AJNR Am J Neuroradiol* 2002;23:1524–1532
38. Taveras JM, Wood EH. *Diagnostic Neuroradiology.* Baltimore: Williams and Wilkins,1964
39. **The nervous system.** In: Moore KL, Persaud TVN. *The Developing Human: Clinically Oriented Embryology.* 6th ed. Philadelphia: W. B. Saunders, 1998:451–489
40. Qureshy A, Kawashima R, Imran MB, et al. **Functional mapping of human brain in olfactory processing: an F-MRI study.** *J Neurophysiol* 2000;84:1656–1666
41. Pritchard TC, Macaluso DA, Eslinger PJ. **Taste perception in patients with insular cortex lesions.** *Behav Neurosci* 1999;113:663–671
42. Riecker A, Ackermann H, Wildgruber D, Dogil G, Grodd W. **Opposite hemispheric lateralization effects during speaking and singing at motor cortex, insula and cerebellum.** *Neuroreport* 2000; 11:1997–2000